Available online at www.sciencedirect.com
ScienceDirect
Journal of Magnetic Resonance 184 (2007) 51–61
JMR Journal of Magnetic Resonance
www.elsevier.com/locate/jmr

The influence of nitrogen-15 proton-driven spin diffusion on the measurement of nitrogen-15 longitudinal relaxation times

Nicolas Giraud [a], Martin Blackledge [c], Anja Böckmann [b], Lyndon Emsley [a,*]

[a] Laboratoire de Chimie (UMR 5182 CNRS/ENS Lyon), Ecole Normale Supérieure de Lyon, Lyon, France
[b] Institut de Biologie et Chimie des Protéines (UMR 5086 CNRS/UCBL), 69367 Lyon, France
[c] Institut de Biologie Structurale Jean Pierre Ebel (CNRS/CEA/UJF), 41 rue Jules Horowitz, 38027 Grenoble, France

Received 3 August 2006; revised 13 September 2006
Available online 9 October 2006

Abstract

The effect of nitrogen-15 proton-driven spin diffusion on quantitative ^{15}N T_1 measurements in solid proteins is investigated, and the impact on the measurement of dynamic parameters is assessed. A simple model of exchange between neighboring nitrogens is used to reproduce the evolution of ^{15}N spin systems whose longitudinal relaxation rates and exchange rates are compatible with experimental measurements. We show that the induced error in the measured T_1 and its effect on the determination of dynamics parameters is likely to be less than the current experimental error. The use of deuterated protein samples is shown to have a small but sometimes visible effect, and may also considerably slow down or even suppress the exchange of magnetization due to spin diffusion.
© 2006 Elsevier Inc. All rights reserved.

Keywords: MAS; Relaxation

1. Introduction

Many of the key functional aspects of proteins are determined by their flexibility. NMR relaxation measurements have long been established as the primary tool to probe protein dynamics in solution [1]. Recently, solid-state NMR methods to study proteins have made outstanding progress, and relaxation measurements in the solid state now become very attractive as a potential tool to study dynamics, especially since molecular dynamics has long been studied in great detail by solid-state NMR in small- and medium-sized molecular compounds, and therefore methods are well established [2,3]. For the study of internal dynamics in proteins, solid-state NMR relaxation appears particularly well adapted, since there is no overall molecular tumbling motion to obscure the effects of the internal motions that are of interest.

Indeed, nitrogen-15 and deuterium have been shown to provide probes for the study of internal mobility along the protein backbone in solid, labeled proteins [4–10]. We have recently shown that ^{15}N longitudinal relaxation times can be measured, and that they provide a qualitative correlation with expected backbone dynamics [8]. We then proposed a detailed analysis of nitrogen-15 spin–lattice relaxation in microcrystalline proteins, with an explicit average sum (EAS) formalism which extends pioneering early work, by Torchia and Szabo [11] and by McDowell and co-workers [12], to the case of restricted N–H bond motions in microcrystalline proteins [9]. We then used it to quantitatively interpret relaxation times in terms of motional amplitudes and characteristic timescales, using a diffusion in a cone model to describe the dynamics of the ^{15}N–^{1}H vectors in the microcrystalline protein Crh based on T_1 data acquired at two different fields [9].

In this paper, we consider the potential perturbation on ^{15}N T_1 measurements due to ^{15}N spin diffusion in ^{15}N-labeled proteins. Notably, we observed a dispersion in the distribution of relaxation rates (up to a factor 7) despite

* Corresponding author. Fax: +33 4 72 72 88 60.
E-mail address: lyndon.emsley@ens-lyon.fr (L. Emsley).

1090-7807/$ - see front matter © 2006 Elsevier Inc. All rights reserved.
doi:10.1016/j.jmr.2006.09.015

the presence of ^{15}N spin diffusion which could tend to equalize the observed decay times. This indicates a minor contribution of this mechanism to the decay of nitrogen-15 magnetization. Nevertheless, a better understanding of the contribution of spin diffusion to longitudinal relaxation is necessary for a rigorous estimation of experimental uncertainty.

Whereas in solution spin diffusion refers to incoherent cross-relaxation, in the solid state it is due to coherent dipole coupling processes [13–17], and depends on the details of the spin network [13,18], at a molecular level and beyond. We focus here on spectral spin diffusion in a solid under MAS, which arises from so-called zero-quantum "flip-flop" transitions [19]. For carbon-13 and nitrogen-15 spin diffusion, diffusion between non-equivalent spins, which should in principle be forbidden, is mediated by the proton spin bath which causes a dipolar splitting of energy levels. As a result, only nuclei within a few angstroms of each other are involved in the exchange process. A combined analysis of ^{13}C–^{13}C and ^{15}N–^{15}N spin-diffusion MAS spectra, recorded on microcrystalline protein samples, has been proved to lead to a useful set of distance constraints: in this context, Castellani et al. [20] determined a structural ensemble which satisfyingly describes the fold of the protein SH3 (although the use of several samples with a combination of different specific labeling schemes was a crucial step in the extraction of structural information from complex, multidimensional spectra). The influence of the MAS speed on ^{15}N spin-diffusion rate has also been recently studied by Krushelnitsky et al. [21].

Here we will not study in detail the structural information contained in nitrogen-15 spin diffusion. We are rather concerned with the perturbing effect it could have on quantitative T_1 measurement. A precise analysis of relaxation

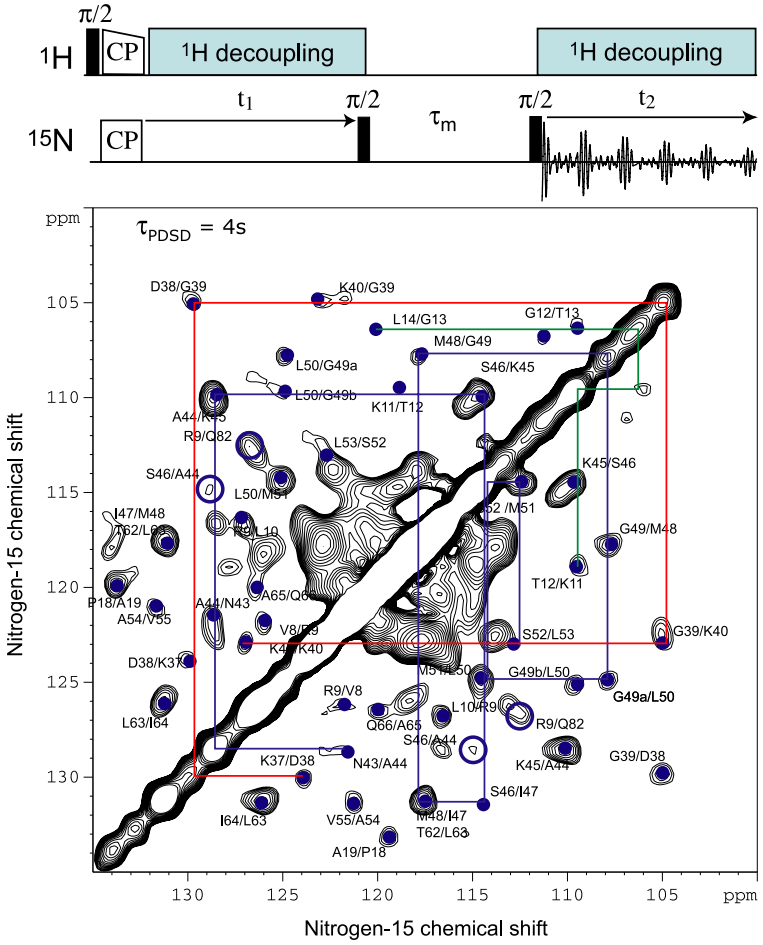

Fig. 1. The 2D ^{15}N–^{15}N spin-diffusion pulse sequence, as well as the resulting correlation spectrum recorded on about 7 mg of Crh. The sample temperature was set to 0 °C, and the rotor spinning speed to 10 kHz. The mixing time (τ_m) is 4 s. Proton decoupling was achieved using the SPINAL-64 decoupling scheme, with a 75 kHz RF field on the proton channel. The experiment was recorded with a maximum indirect acquisition time $t_{1max} = 14.03$ ms, and a direct acquisition time of 20 ms. Each increment in t_1 was acquired with 128 scans, and the spectral width in both dimensions is 18 kHz. Data were processed with zero filling and a $\cos^2$ filter. The assignment of the nitrogen-15 proton-driven spin-diffusion spectrum is also shown: crosspeaks which could be assigned to two neighboring nitrogens are labelled according to the residues involved. Three sequential walks are shown involving residues K11–L14 (green), K37–K41 (red) and N43–L53 (blue). Finally, we show two non-sequential correlations which correspond to the S46–A44 pair, and the intermonomer contact R9–Q82 (open blue circles). The simulation of sequential correlations of nitrogens $^{15}N^{(i)}$ with their neighbors $^{15}N^{(i-1)}$ and $^{15}N^{(i+1)}$ (for the sake of the readibility of this figure, we only plot the resolved simulated contacts) is also shown (filled blue circles). (For interpretation of the references to color in this figure legend, the reader is referred to the web version of this paper.)

curves reveals perturbations on a time scale (1 s) which is short compared to the relaxation regime (tens of seconds). Spin diffusion can be slowed somewhat (but not fully quenched) by dilution of the proton bath upon deuteration. In this paper, we develop and study a simple model to describe ^{15}N spin diffusion during longitudinal relaxation experiments, based on our experimental observations on a microcrystalline, uniformly labeled sample of the protein Crh, and we estimate the deviation in relaxation measurements which could be induced by this mechanism for various initial conditions: we first evaluate experimentally how many nitrogens are typically involved in a spin-diffusion process, on a time scale relevant to the study of longitudinal relaxation, and we estimate the exchange rate σ which characterizes the transfer between two unlike spins i and j, without making any assumption on its dependence on experimental parameters [22,23]. According to these experimental observations, we then use a simplified relaxation matrix protocol to characterize the uncertainty which is introduced into the dynamics parameters determined through nitrogen-15 spin–lattice relaxation.

2. Analysis of the ^{15}N spin-diffusion spectrum for Crh

In order to evaluate ^{15}N–^{15}N spin-diffusion rates in our Crh sample, and probe on which spatial scale this phenomenon can interfere with longitudinal relaxation, we have recorded a 2D, ^{15}N–^{15}N proton-driven spin-diffusion experiment under MAS, on a microcrystalline, uniformly labeled [^{15}N,^{13}C] sample of the protein Crh in its dimeric form [24]. We have set the spin-diffusion time τ_m to 4 s (which is the same as the delay chosen by Castellani et al. [25] for the SH3 sample). In Fig. 1, we show the spectrum which was recorded at 10 kHz spinning speed. We assigned resolved cross-signals in this spectrum by comparison to the simulation of a set of short to long distance ^{15}N–^{15}N correlation experiments, generated from the nitrogen-15 chemical shifts determined by Böckmann et al. [26].

An analysis of the resolved contacts shows that nitrogen-15 magnetization is mainly transferred from one given ^{15}N spin to its nearest neighbors, for a mixing time of 4 s. Sequential walks, which link residues in the order according to the protein sequence, could be identified for three stretches of residues involving K11–L14, K37–K41, and N43–L55. Nevertheless, most of the sequential cross-peaks are located in the non-resolved region of the spectrum, between 112 and 125 ppm. The observation of sequential contacts is coherent with results which were obtained for the same experiment on SH3: for the same mixing time, on a doubly labeled [^{2}H,^{15}N] sample of this protein, Reif et al. [22] essentially observe sequential cross-peaks along the backbone. A few non-sequential correlations could also be identified, through the combined use of both the nitrogen-15 chemical shift assignment and the 3D structure of the Crh dimer (PDB entry 1mu4) [24]. For instance, for the assignment of a cross-peak between Ser 46 and Ala 44, we predict a 4.3 Å distance from the crystal structure,

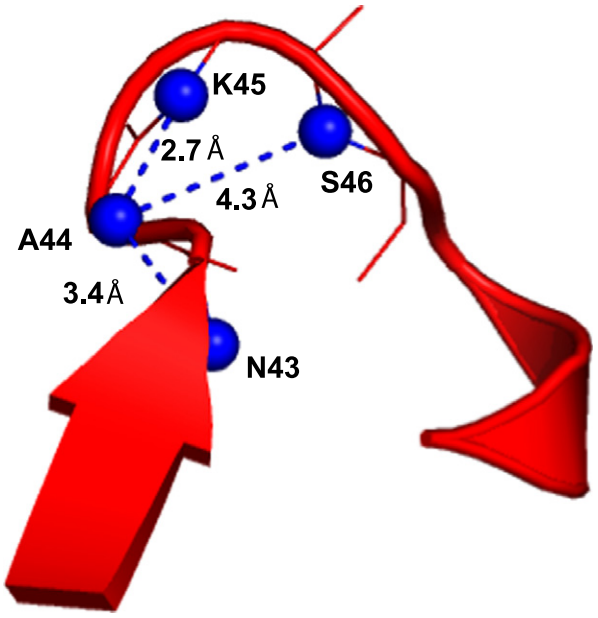

Fig. 2. Representation of the crystallographic structure of Crh for the residues whose nitrogen-15 gives a correlation with Ala 44. Nitrogen atoms are plotted with blue spheres. For each correlation the distance is indicated. (For interpretation of the references to color in this figure legend, the reader is referred to the web version of this paper.)

which is coherent with the distances observed by Castellani et al. [20] (between 3 and 6 Å—note that the sequential contact which was identified between Ala 44 and Asn 43 corresponds to a distance of 3.4 Å between the two nitrogens, as it is shown in Fig. 2).

Finally, we observe an inter-monomer contact between Arg 9 and Gln 82. This correlation corresponds to a 4.75 Å distance in the crystallographic structure, whereas these two residues within the same chain are far from each other, as can be seen in Fig. 3 (this observation constitutes an additional experimental proof of the dimeric state of the protein in the microcrystalline sample used for solid-state NMR [24]).

3. Consequences of ^{15}N spin diffusion on T_1 measurements

The assignment of the ^{15}N spin-diffusion spectrum reveals transfers which occur over short distances (mainly about 5 Å during a 4 s mixing time), and are essentially sequential (this rather short distance can be explained by the weak dipolar couplings between ^{15}N spins—about six times weaker than between ^{13}C spins for the same distance—and by the more diluted network of nitrogens in a protein, compared to carbons). These observations lead us to propose a simplified description of the nitrogen-15 spin-diffusion mechanism, which we model as a re-equilibration of magnetization between two neighboring ^{15}N spins.

Furthermore, we also have estimated the average exchange rate which characterizes the ^{15}N–^{15}N spin-diffusion process in our sample, under magic angle spinning ($\omega_r = 10$ kHz). Considering sequential cross-peaks whose

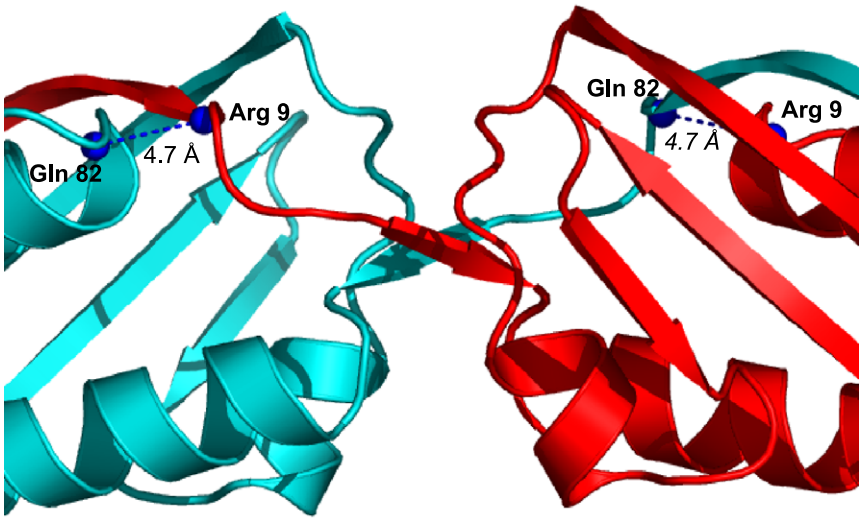

Fig. 3. Residues Arg 9 and Gln 82, whose nitrogens correlate in the ^{15}N–^{15}N spin-diffusion experiment, in the crystallographic structure of Crh [24]. Each monomer is drawn with a different color in order to highlight the interface. Nitrogen atoms from these residues are plotted with blue spheres. (For interpretation of the references to color in this figure legend, the reader is referred to the web version of this paper.)

Table 1
The ratios $I^{\text{cross-peak}}/I^{\text{diagonal}}$ which were measured from the analysis of the ^{15}N–^{15}N spin-diffusion experiment for the residues whose nitrogen-15 chemical shift is resolved in the 1D spectrum

Residue	$I^{\text{cross-peak}}_{N,N+1}/I^{\text{diagonal}}$	$I^{\text{cross-peak}}_{N,N-1}/I^{\text{diagonal}}$
Gly 39	0.14	0.16
Ala 44	0.11	0.02
Asp 38	0.16	0.09
Gly 13	0.04	0.12
Gly 49	0.12	0.09

chemical shifts provide resolved signals (i.e., correspond to a single residue) on the diagonal of the spectrum, we measured the ratio between the intensity of one cross-peak and the intensity of the diagonal (Table 1), and have divided this ratio by the spin-diffusion delay (4 s).

From this analysis, we measure an average intensity ratio $I^{\text{cross-peak}}/I^{\text{diagonal}} \sim 0.10$, and hence an average exchange rate of $\sigma \sim 0.025\ \text{s}^{-1}$. In the following, we use this average rate in order to study qualitatively the possibility of a re-equilibration of the magnetization among neighboring nitrogens during a spin–lattice relaxation period as a mechanism to describe initial deviations in decaying curves.

4. Two spins coupled by spin diffusion

For simplicity, we *assume* that spin diffusion can be described by a system of coupled equations (which is the starting point of the rate matrix analysis) [17,23,27,28]:

$$\frac{\mathrm{d}M_z}{\mathrm{d}t} = -[K+R]\cdot(M_z - M_0), \tag{1}$$

where R is the matrix which accounts for longitudinal relaxation during the mixing time, and K is the kinetic matrix for rates that we use to describe phenomenologically the proton-driven spin-diffusion exchange processes between rare nuclei. In the case of ^{15}N spin diffusion, whose time scale is much slower than that of proton–proton spin diffusion, we a priori *do not* neglect the longitudinal relaxation (since we want to study a possible interference between these two regimes). We note that although their time scale can possibly be similar, the mechanisms of spin diffusion and longitudinal relaxation for a rare nucleus are intrinsically independent: relaxation is notably induced by the random fluctuations of various interactions, mainly due to molecular dynamics, at the Larmor frequency, whereas spin diffusion occurs even in a static system, and is caused by coherent dipolar exchange processes with a time scale which is imposed by the effective strength of the dipolar bath.

We consider two nitrogens, I and S, whose initial polarization can be different, and whose longitudinal relaxation rates are, respectively, R_1^I and R_1^S, which are equilibrating with an exchange rate σ. We obtain

$$\frac{\partial}{\partial t}\begin{bmatrix} I \\ S \end{bmatrix} = -(K+R)\cdot\left(\begin{bmatrix} I \\ S \end{bmatrix} - \begin{bmatrix} M^0 \\ M^0 \end{bmatrix}\right), \tag{2}$$

where $K = \begin{bmatrix} -\sigma & \sigma \\ \sigma & -\sigma \end{bmatrix}$ and $R = \begin{bmatrix} R_1^I & 0 \\ 0 & R_1^S \end{bmatrix}$. The equations that describe the evolution for this system thus read:

$$\begin{aligned} \frac{\partial I}{\partial t} &= -R_1^I(I - M^0) - \sigma(I - S), \\ \frac{\partial S}{\partial t} &= -R_1^S(S - M^0) - \sigma(S - I), \end{aligned} \tag{3}$$

where M^0 is the nitrogen magnetization at thermal equilibrium. Using a change of variables $x(t) = I(t) - M^0$, $y(t) = S(t) - M^0$, $A = R_1^I + \sigma$ and $B = R_1^S + \sigma$, we obtain an equivalent system:

$$\begin{aligned}\frac{\partial x}{\partial t} + Ax - \sigma y = 0,\\ \frac{\partial y}{\partial t} + By - \sigma x = 0,\end{aligned} \tag{4}$$

which has a second-order determinant. Initial conditions are defined as $x(t=0) = x^0$, $y(t=0) = y^0$, and the solution of this system is:

$$\begin{aligned}x(t) &= (x^0 - C^x)\,\mathrm{e}^{-\lambda_+ t} + C^x\,\mathrm{e}^{-\lambda_- t},\\ y(t) &= C_1^y \cdot \mathrm{e}^{-\lambda_+ t} + C_2^y \cdot \mathrm{e}^{-\lambda_- t},\end{aligned} \tag{5}$$

where the constants C_x, C_1^y, C_2^y, and $\lambda_\pm$ verify:

$$C^x = \frac{\sigma y^0 - \lambda_+ x^0}{\sqrt{\Delta}},$$

$$C_1^y = \frac{(A-\lambda_+)}{\sigma}(x^0 - C^x),$$

$$C_2^y = \frac{(A-\lambda_-)}{\sigma}C^x,$$

$$\lambda_\pm = \tfrac{1}{2}(A + B \pm \sqrt{\Delta}),$$

and $\Delta = A^2 - 2AB + B^2 + 4\sigma^2$.

5. Simulations

We used the Maple software [29] to simulate the time dependence of the magnetization of spins I and S, in order to estimate the effective relaxation rates using various parameters. The impact of magnetization exchange between nitrogens on T_1 relaxation measurements is evaluated by fitting the curves predicted in our simulations to single exponential curves with effective relaxation rates $R^I_{1\mathrm{eff}}$ and $R^S_{1\mathrm{eff}}$, and determining the difference between $R_{1\mathrm{eff}}$ and the actual R_1.

In Fig. 4, we show the deviation $|R^I_1 - R^I_{1\mathrm{eff}}|$ which is observed for various initial magnetizations and relaxation rates. The spin-diffusion rate is set to its experimentally determined average value of 0.025 s^{-1}, and the longitudinal relaxation rate of the I spin to an average value of 0.08 s^{-1}.

We observe that the deviation is generally smaller than 0.01 s^{-1}, except when the I spin is both much less polarized initially (by about a factor 2), and relaxes much faster than the S spin. Nevertheless, this deviation stays within the current experimental uncertainty.

To complete the study, in Table 2 we show the results of some additional simulations with different initial conditions. In particular, we have studied to what extent the combination of differences in initial magnetization and spin-diffusion rates together with very different relaxation rates can induce a deviation in the measurement of spin–lattice relaxation.

We observe that the deviation in the measurement of R_1 is mainly dependent on the initial difference in polarization between the two sites which are exchanging magnetization. However, this deviation is really critical in only one typical case: if the spin-diffusion rate is about 10 times faster than the rate that we have measured experimentally (*e.g.*, $\sigma \sim 0.25\ \mathrm{s}^{-1}$), then the magnetization transfer between the two nitrogens would be fast enough to impose the same evolution for both nuclei which would therefore show almost the same apparent relaxation curve. Nevertheless, in this case it would not be possible to observe any differences of the relaxation rates from site to site. This analysis also shows us that the influence of the equilibration process on relaxation measurement is weaker if we record relaxation data on longer delays rather than on the very first seconds, which corresponds to the protocol that we have used experimentally so far.

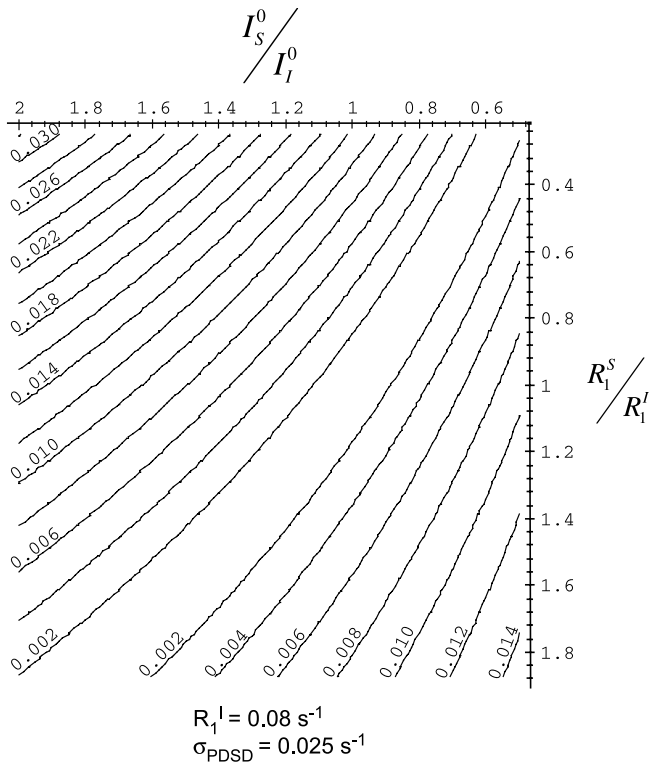

Fig. 4. Contour plot of the difference $|R^I_1 - R^I_{1\mathrm{eff}}|$ (in s^{-1}) as a function of initial polarization difference and the relaxation rates of the nitrogen-15 spins I and S. R_1^{eff} is calculated by least-square fitting with a monoexponential function of the simulated non-exponential relaxation curve, from four points (at 1, 4, 7 and 15 s, which correspond to a standard experimental procedure).

Table 2
Influence of ^{15}N spin diffusion between two sites with different initial magnetization

$I(0)/M^0$	$S(0)/M^0$	σ (s^{-1})	R^I_1 (s^{-1})	$R^I_{1\mathrm{eff}}$ (s^{-1})	R^S_1 (s^{-1})	$R^S_{1\mathrm{eff}}$ (s^{-1})
2.5	1.5	0.025	0.12	**0.124**	0.04	**0.031**
2.5	1.5	0.025	0.04	**0.053**	0.04	**0.013**
2.5	1.5	0.025	0.12	**0.133**	0.12	**0.093**
2.5	2.5	0.025	0.12	**0.103**	0.04	**0.049**
2.5	1.5	0.0025	0.12	**0.121**	0.04	**0.038**
2.5	1.5	0.01	0.12	**0.123**	0.04	**0.035**
2.5	1.5	0.05	0.12	**0.123**	0.04	**0.031**
2.5	1.5	0.25	0.12	**0.1**	0.04	**0.053**
2.5	1.5	0.025	0.04	**0.057**	0.12	**0.064**

For each set of initial conditions, the effective relaxation rates that would be measured from the resulting decaying curves by fitting them with a mono-exponential function are shown in bold.

Fig. 5 shows the evolution of the magnetization when the I spin is initially both the most polarized spin and has the fastest relaxation rate. In this case, we even observe that the magnetization from the S spin grows slightly in the very first seconds, as a result of the contribution from the magnetization transfer. This situation, which correspond to a set of reasonably realistic initial conditions, reproduces some initial behaviors which we observed experimentally for some residues in the protein Crh (data not shown here). However, even in this case, the effective relaxation rates which would be measured are close to the "pure" spin–lattice relaxation rates.

In the opposite case, where the spin which is initially the most polarized undergoes the slowest relaxation, both decaying curves are modified, and we can see that the equilibration mechanism tends to homogenize the evolution of both curves (Fig. 6).

As a result, in this case this equilibration induces a stronger deviation from "pure" relaxation rates. Even so, except in some pathological situations, this deviation is negligible with respect to current experimental uncertainty.

Furthermore, Fig. 7 illustrates to what extent the determination of dynamics parameter in proteins, through the measurement of longitudinal relaxation rates at two different fields, could be affected by the local nitrogen-15 spin diffusion.

In Fig. 7a, the dynamics determined from curves including ^{15}N spin diffusion is very close to that which would be found for "pure" spin–lattice relaxation. This suggests that the contribution of a re-equilibration process does not change fundamentally the quality of the dynamic information which is present in this kind of relaxation data. Nevertheless, in Fig. 7b we can see that in another range of dynamics which corresponds to rather "rigid" residues (within the diffusion in a cone model), nitrogen-15 spin diffusion apparently has a stronger effect on the determination of dynamics, even though the curves corresponding to a given value of the relaxation rate are not changed much: this comes from the intrinsic difficulty to theoretically constrain the motional model from longitudinal relaxation rates measured at two different fields in this dynamic regime.

Furthermore, in Fig. 8 we compare the deviation in the determination of dynamics resulting from the incursion of ^{15}N spin diffusion, to the dynamic probability distributions $P(\tau_W, \theta_0)$ which were calculated from experimental data recorded on Crh [9]. We recall that $P(\tau_W, \theta_0)$ is a combined function of the quality of the experimental data (i.e., the

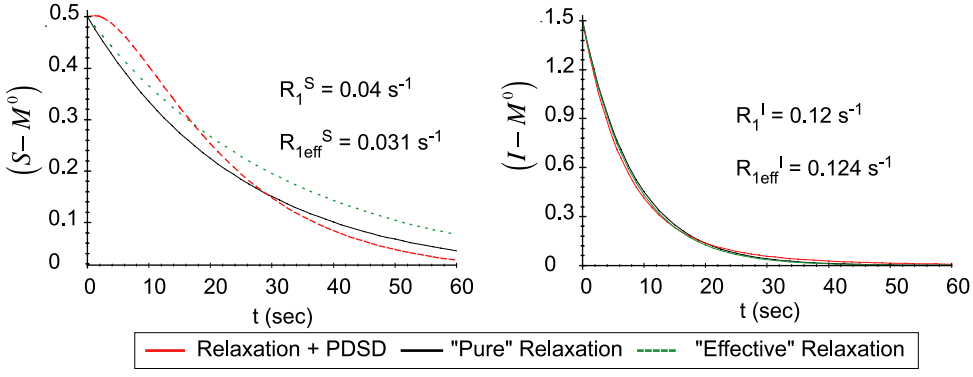

Fig. 5. Typical evolution of magnetization for spins I and S, for the following initial conditions: $I(0) = 2.5 \times M^0$, $S(0) = 1.5 \times M^0$, $\sigma = 0.025\ s^{-1}$, $R_1^I = 0.12\ s^{-1}$, $R_1^S = 0.04\ s^{-1}$. Nitrogen-15 magnetization is displayed in an arbitrary unit so that $M^0 = 1$. The solid lines ("Relaxation") represent the monoexponential relaxation curve $N^0 \exp(-R_1^N \cdot t)$, with $N = I$ or S spin. The dashed lines ("Relaxation + PDSD") represent the simulated curves which account for both spin–lattice relaxation and magnetization exchange, and the second type dashed lines (""Effective" relaxation") represent the monoexponential curves which best fit the magnetization decays in presence of spin diffusion.

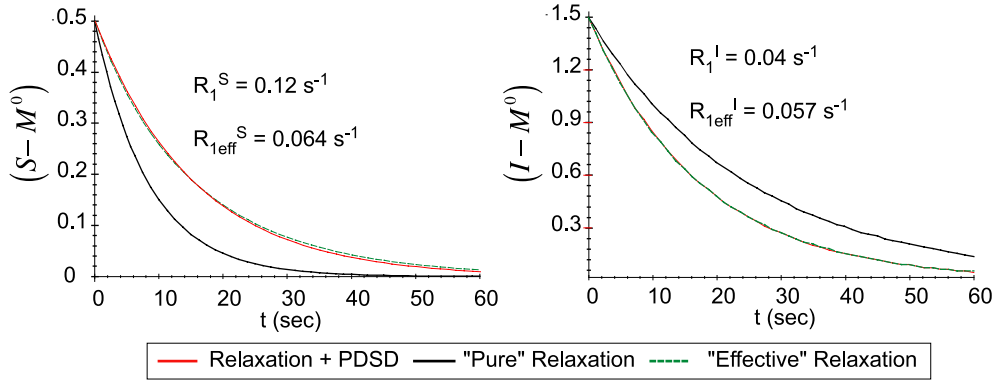

Fig. 6. Decaying curves for spins I and S in the following initial conditions: $\sigma = 0.025\ s^{-1}$, $I(0) = 2.5 \times M^0$, $S(0) = 1.5 \times M^0$, $R_1^I = 0.04\ s^{-1}$, $R_1^S = 0.12\ s^{-1}$. The displayed curves are of the same type described in Fig. 5.

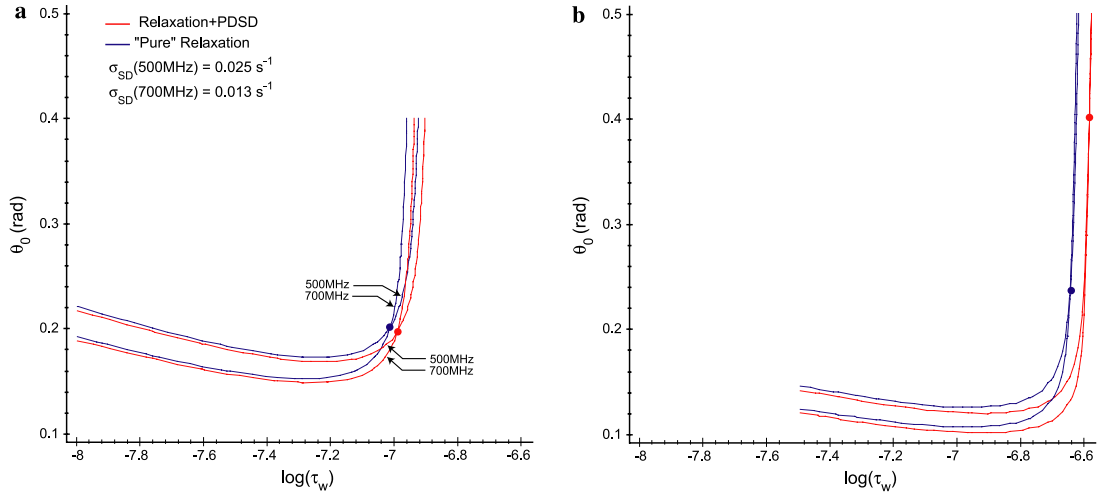

Fig. 7. Simulation of the determination of the dynamic parameters for a nitrogen-15 (a) from a "flexible" residue and (b) from a "rigid" residue, from the measurement of ^{15}N longitudinal relaxation rates measured at proton frequencies of 500 and 700 MHz, for "pure" spin–lattice relaxation (blue curves), and with a contribution from nitrogen-15 spin diffusion with a neighboring site (red curves). The relaxation rates which were measured using an EAS approach [9], were back-calculated so that the dynamic parameters determined from the decaying curves including the contribution of spin diffusion correspond to those which were experimentally found (a) for Asp 38, and (b) for Lys 41 in microcrystalline Crh [9]. The ^{15}N spin-diffusion rate was set to 0.025 s^{-1} at 500 MHz (we assume that this average value is roughly the same for each residue in Crh), and consequently estimated to be 0.013 s^{-1} at 700 MHz. In order to simulate the spin–lattice relaxation of the nitrogen-15 nucleus, we assume that spin–lattice relaxation is dominated by the fluctuations of the dipolar interaction between the nitrogen and its bound proton in the amide group, and that the internal motion of the N–H interaction vector is described by the model of diffusion in a cone, with a diffusion time τ_W, and a cone of semi-angle θ_0. For the spin-diffusion partner we simply assume that initial magnetization is equal to that of the studied nitrogen-15. (For interpretation of the references to color in this figure legend, the reader is referred to the web version of this paper.)

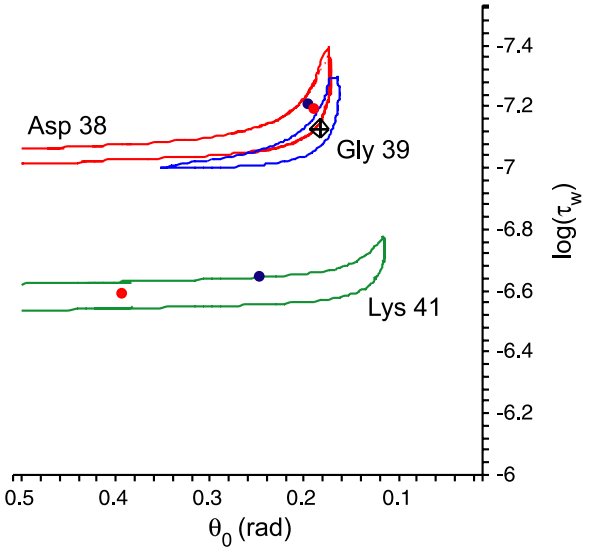

Fig. 8. Contour plots of $P(\tau_W, \theta_0)$ for three residues: Asp 38 (red), Gly 39 (blue), and Lys 41 (dark green) (for each distribution, only the contour corresponding to $P(\tau_W, \theta_0) = 0.9 \times P_{MAX}$ is plotted, with P_{MAX} the maximum value of each function $P(\tau_W, \theta_0)$). $P(\tau_W, \theta_0)$ measures the deviation between experimentally determined relaxation rates and the best fit for the determination of dynamic parameters. For Asp 38 and Lys 41, the dynamics which could be determined either from a "pure" longitudinal relaxation description (blue circles) or by accounting for a contribution from spin diffusion (red circles), are superimposed to these distributions. For Gly 39, the position of P_{MAX} is represented by a black diamond. (For interpretation of the references to color in this figure legend, the reader is referred to the web version of this paper.)

error in R_1), and the resolution with which a given dynamic behavior can be determined through the observation of a crossing of curves from relaxation measurements at two different fields.

We observe that although the dynamics determined for Asp 38 accounting for ^{15}N spin diffusion is slightly different from the determination which results from a "pure" relaxation approach, nevertheless the determination in any case is still localized within the 90% probability distribution which was calculated from the experimental data, and still allows us to make a clear distinction between the dynamics of Asp 38 and Gly 39 despite their respective mobilities being similar. Moreover, for Lys 41, the dynamics determined by including a contribution from ^{15}N spin diffusion in our analysis is again localized within the 90% probability distribution, though it yields a substantially different value of the angle θ_0 compared to the "pure" relaxation approach. This observation shows that the effective contribution of nitrogen-15 spin diffusion to the deviation in the determination of dynamics mostly depends, as for any other source of experimental uncertainty, on the intrinsic difficulty to sample, for certain kinds of dynamics, spectral densities with only one relaxation rate measured at two different fields, for a given motional model. This difficulty could be avoided by constraining the motional model with a relaxation rate complementary to R_1 (like, for instance, cross-relaxation rates), which could be measured from other experiments in the future.

6. Three-spin system

The model used above to evaluate the influence of nitrogen-15 spin diffusion on ^{15}N R_1 measurements described local re-equilibration of magnetization between two neighboring sites, and is thus based on a two-spin system. We now briefly consider the case of a nitrogen-15 which can exchange magnetization with the two neighboring nitrogens from both adjacent peptide bonds. Equations that describe the evolution for this system read:

$$\begin{aligned}\frac{\partial N^{(i)}}{\partial t} &= -R_1^{(i)}(N^{(i)} - M^0) - \sigma(N^{(i)} - N^{(i+1)}) \\ &\quad - \sigma(N^{(i)} - N^{(i-1)}), \\ \frac{\partial N^{(i+1)}}{\partial t} &= -R_1^{(i+1)}(N^{(i+1)} - M^0) - \sigma(N^{(i+1)} - N^{(i)}), \\ \frac{\partial N^{(i-1)}}{\partial t} &= -R_1^{(i-1)}(N^{(i-1)} - M^0) - \sigma(N^{(i-1)} - N^{(i)}).\end{aligned} \tag{6}$$

If we consider the change of variables: $I = N^{(i)}$, $S = N^{(i+1)} + N^{(i-1)}$, $R_1^I = R_1^{(i)}$, $R_1^S = R_1^{(i+1)} + R_1^{(i-1)}$, we obtain:

$$\begin{aligned}\frac{\partial I}{\partial t} &= -R_1^I(I - M^0) - \sigma(2I - S), \\ \frac{\partial S}{\partial t} &= -R_1^S(S - 2M^0) - \sigma(S - 2I).\end{aligned} \tag{7}$$

We can see that the case of a three-spin system is equivalent to that of a virtual two-spin system. If we consider the following change of variables (note that this time we have to account for twice the spin-diffusion rate in the constant A):

$$x(t) = I(t) - M^0, \quad y(t) = S(t) - 2M^0, \quad A = R_1^I + 2\sigma, \quad B = R_1^S + \sigma.$$

We have:

$$\begin{aligned}\frac{\partial x}{\partial t} + Ax - \sigma y &= 0, \\ \frac{\partial y}{\partial t} + By - \sigma x &= 0.\end{aligned} \tag{8}$$

In Fig. 9, we show the deviation $|R_1^I - R_{1\text{eff}}^I|$ as a function of the initial magnetizations and relaxation rates of $I(t)$ and the virtual system $S(t)$. As previously, the spin-diffusion rate σ is set to 0.025 s^{-1}, and the longitudinal relaxation rate of the I spin to 0.08 s^{-1}.

Fig. 9 shows that for "realistic" initial conditions, the deviation is generally comparable to what was predicted using the simple two-spin model: it is generally smaller than 0.02 s^{-1}. This observation is coherent with the assumption of a local re-equilibration (whatever the number of spins involved) of the magnetization among nitrogens as a plausible process to quantitatively reproduce the deviation which is observed for ^{15}N spin–lattice relaxation curves. However, under these conditions, the deviation in the determination of dynamics which is introduced by this phenomenon does not modify the dynamic probability distributions whose width is mostly dominated by the ability to constrain the motional model with a given set of relaxation rates.

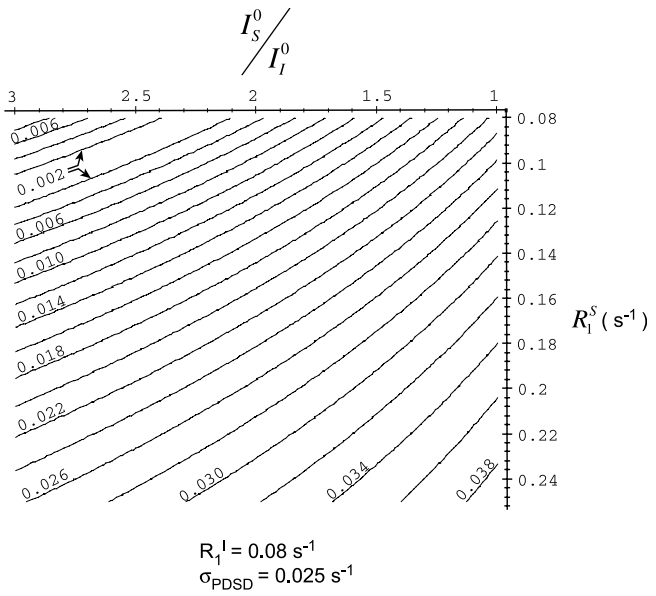

Fig. 9. Plot of the difference $|R_1^I - R_{1\text{eff}}^I|$ (in s^{-1}) as a function of initial polarization and relaxation rates of the nitrogen-15 spin I and the virtual two-spin system S. The parameters are the same as for Fig. 4.

7. Influence of the dipolar ^{15}N field

The analysis of these simulations shows that the observed initial non-exponential behavior of nitrogen-15 longitudinal relaxation curves can be explained by an exchange model between nitrogens. However, only two (or three) sites are considered in order to interpret data. In principle, one could argue that more ^{15}N spins could participate, and that relaxation times may reflect the local density in nitrogens, around a given site.

Although there is no support for this in the proton-driven spin-diffusion spectrum (where we mainly see sequential contacts), we have nevertheless looked for a possible correlation between ^{15}N R_1s measured for Crh (at 11.74 T) [8], and the quantity $\sum_{r_{\text{NN}}<8\ \text{angst}}(1/R_{\text{NN}}^6)$, calculated from the crystallographic structure [24], and which loosely represents a sort of "dipolar field" generated by nitrogens located within a 8 Å radius from the ^{15}N spin whose T_1 is measured (Fig. 10).

We see no correlation between the longitudinal relaxation rate and the nitrogen density along the backbone. This suggests that the equilibration process is effectively local and limited to a few pairs of nitrogens.

8. Nitrogen-15 spin–lattice relaxation measured in deuterated Crh

Another possible source of interference in the dynamic analysis could be the contribution to T_1 relaxation from neighboring, but not attached, protons. To evaluate this,

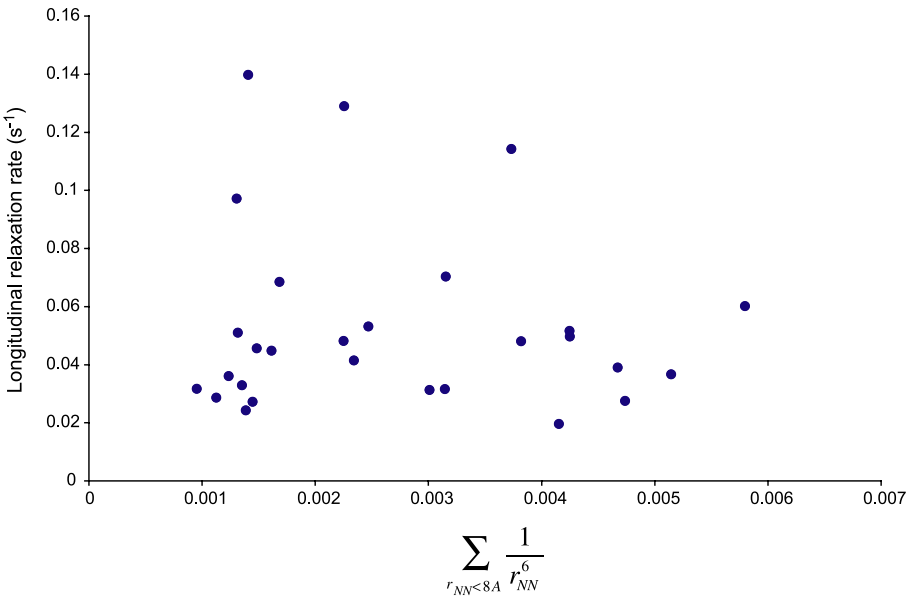

Fig. 10. A plot of nitrogen-15 longitudinal relaxation rates measured for microcrystalline Crh at 11.74 T [8], as a function of the dipolar field ^{15}N. Each point corresponds to one of the 28 residues which were studied.

we have measured R_1s in a deuterated form of Crh [30–32], and they are reported in Table 3. Fig. 11 shows the comparison between R_1s measured with and without the contribution of the proton bath surrounding amide groups.

Table 3
Longitudinal relaxation rates measured on a microcrystalline, uniformly labeled [^{15}N,^{13}C] sample of the Crh protein, at 500 MHz proton frequency, as well as the difference with the same rates measured for the protonated sample under identical experimental conditions

Residue	R_1^{2H} (s^{-1})	$R_1^{2H} - R_1^{1H}$ (s^{-1})
Val 8	0.031	−0.037
Gly 13	0.033	−0.013
Leu 14	0.013	−0.016
Val 23	0.015	−0.013
Asp 38	0.035	−0.094
Gly 39	0.105	−0.009
Lys 41	0.056	0.005
Ala 44	0.042	−0.006
Lys 45	0.021	−0.039
Ile 47	0.038	0.006
Gly 49	0.036	−0.012
Leu 50	0.038	−0.003
Met 51	0.022	−0.005
Ser 52	0.055	0.002
Ala 54	0.042	−0.098
Gly 58	0.020	−0.012
Leu 63	0.019	−0.026
Ile 64	0.008	−0.019
Ala 65	0.019	−0.014
Gly 67	0.034	0.010
Asp 69	0.030	−0.022
Tyr 80	0.025	−0.014
Val 81	0.056	0.006
Gln 82	0.030	−0.007

An estimation of the experimental uncertainty was calculated for each residue in both samples, using the protocol described elsewhere [9]: the average standard deviation in R_1 was found to be 0.018 s^{-1} in protonated Crh and 0.011 s^{-1} in deuterated Crh.

We note that the relaxation times are in general slightly, but not dramatically, increased for most of the resonances. We observe that despite the relatively poor accuracy of these measurements [8] (for instance, the signal which led to the study of residue Val 8 is very weak), we do detect for four residues (Val 8, Asp 38, Lys 45, and Ala 54) a significant variation in ^{15}N R_1s (residues shown in red in Fig. 11). This variation could either be due to the suppression of nitrogen-15 PDSD in the deuterated sample or to the suppression of secondary relaxation mechanisms from non-bonded protons. However, the details of the quantitative correlation between deuteration, the modification of relaxation and spin diffusion, and dynamics, are currently hard to determine, and we can only observe that these four residues are all located in mobile loops in the protein. For the moment, we simply conclude that it appears at the current level of accuracy that deuteration is probably not essential, though it may well be useful in the future if the precision of these experiments increases substantially.

9. Conclusion

We have considered the effect that proton-driven spin diffusion may have on quantitative ^{15}N T_1 measurements in solid proteins. A simple model of exchange between neighboring nitrogens allows us to reproduce the observed evolutions for ^{15}N spin systems whose longitudinal relaxation rates and exchange rates are compatible with experimental measurements ($R_1 \sim 0.08\ s^{-1}$, $\sigma \sim 0.025\ s^{-1}$). The analysis of this model shows that the existence of inhomogeneities in magnetization between neighboring sites in the protein is the main driving force of this exchange process. We show that the induced error in the measured T_1 and its effect on the

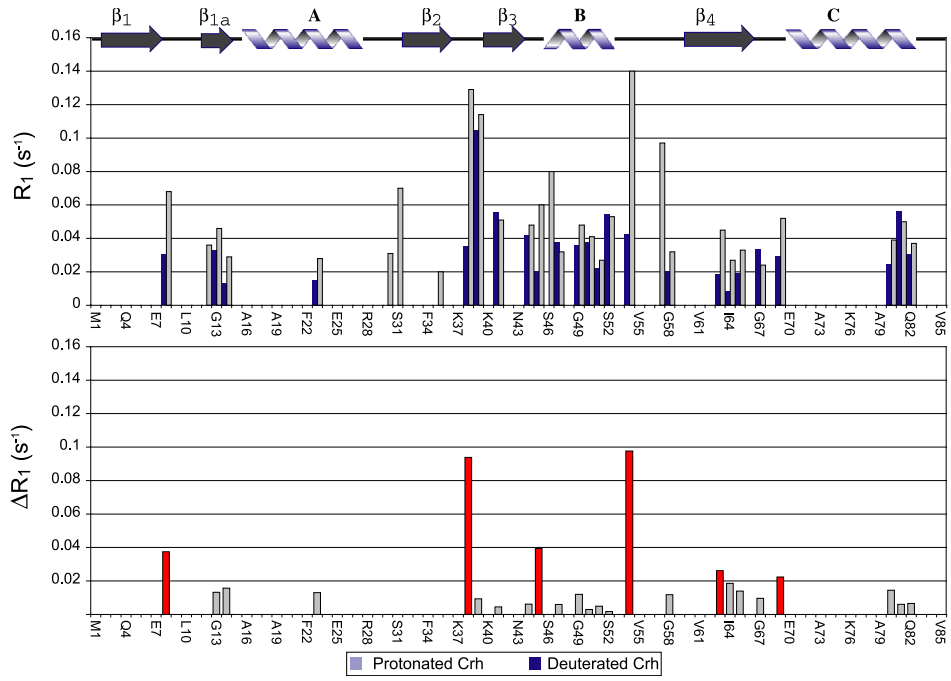

Fig. 11. (Top) A bargraph of longitudinal relaxation rates measured on protonated (grey) and deuterated (blue) samples of Crh vs residue position. (Bottom) The deviation in R_1, $|R_1^{1H} - R_1^{2D}|$ between the protonated and the deuterated form. The secondary structure of the dimeric form of the protein Crh is shown above. Values are given in Table 3. Experiments were carried out on a Bruker Avance 500 MHz spectrometer using a 4 mm triple tuned CP-MAS probe, at a spinning speed of 10 kHz using the protocol described elsewhere [8]. (For interpretation of the references to color in this figure legend, the reader is referred to the web version of this paper.)

determination of dynamics parameters is likely to be less than the current experimental error. However, in order to avoid any critical cases we recommend that ^{15}N T_1 measurements should be routinely accompanied by verification of the ^{15}N–^{15}N proton-driven spin-diffusion behavior.

The inhomogeneity in magnetization throughout the protein is mainly due to the nature of the transfer step from protons to nitrogens through cross-polarization (CP). Many options could thus allow one to avoid a perturbation of the data by spin diffusion. On the one hand, measuring another relaxation rate (than R_1) would provide a better sampling of spectral densities, as well as a measurement which may be less sensitive to re-equilibration. On the other hand, more simply fast MAS experiments should rapidly quench ^{15}N–^{15}N proton-driven spin diffusion, and lead to "pure" spin–lattice relaxation measurements. In view of the rates measured here, we estimate that in most proteins spin diffusion could be completely neglected for spinning rates above around 20 kHz (although we note that very high precision measurements of long relaxation times in the future would continue to be slightly affected even by very slow spin diffusion). Uniform ^{1}H–^{15}N CP methods would also reduce the amplitude of this effect. Finally, we have shown that the use of deuterated protein samples has a small but sometimes visible effect, and may also considerably slow down—or even suppress—the exchange of magnetization due to spin diffusion.

References

[1] A. Mittermaier, L.E. Kay, Review—New tools provide new insights in NMR studies of protein dynamics, Science 312 (5771) (2006) 224–228.
[2] R. Vold, R.L. Vold, Deuterium relaxation in molecular solids, in: W.S. Warren (Ed.), Advances in Magnetic and Optical Resonance, Academic Press, New York, 1991, p. 85.
[3] H.W. Spiess, Rotation of molecules and nuclear spin relaxation, in: P. Diehl, E. Fluck, R. Kosfeld (Eds.), NMR Basic Principles and Progress, Springer-Verlag, Berlin, Heidelberg, New York, 1978, p. 15.
[4] H.B.R. Cole, D. Torchia, An NMR study of the backbone dynamics of staphylococcal nuclease in the crystalline state, Chem. Phys. 158 (2–3) (1991) 271–281.
[5] A.C. Wang, M.A. Kennedy, B.R. Reid, G.P. Drobny, A solid-state H-2-Nmr investigation of purine motion in a 12-base-pair RNA duplex, J. Magn. Reson. B 105 (1) (1994) 1–10.
[6] J.W. Mack, M.G. Usha, J. Long, R.G. Griffin, R.J. Wittebort, Backbone motions in a crystalline protein from field-dependent H-2-NMR relaxation and line-shape analysis, Biopolymers 53 (1) (2000) 9–18.
[7] S. Rozovsky, A.E. McDermott, The time scale of the catalytic loop motion in triosephosphate isomerase, J. Mol. Biol. 310 (1) (2001) 259–270.
[8] N. Giraud, A. Böckmann, A. Lesage, F. Penin, M. Blackledge, L. Emsley, Site-specific backbone dynamics from a crystalline protein by solid-state NMR spectroscopy, J. Am. Chem. Soc. 126 (37) (2004) 11422–11423.
[9] N. Giraud, M. Blackledge, M. Goldman, A. Böckmann, A. Lesage, F. Penin, L. Emsley, Quantitative analysis of backbone dynamics in a crystalline protein from nitrogen-15 spin–lattice relaxation, J. Am. Chem. Soc. 127 (51) (2005) 18190–18201.
[10] M. Hologne, Z.J. Chen, B. Reif, Characterization of dynamic processes using deuterium in uniformly H-2, C-13, N-15 enriched peptides by MAS solid-state NMR, J. Magn. Reson. 179 (1) (2006) 20–28.

[11] D. Torchia, A. Szabo, Spin–lattice relaxation in solids, J. Magn. Reson. 49 (1982) 107–121.
[12] A. Naito, S. Ganapathy, K. Akasaka, C.A. McDowell, Spin–lattice relaxation of C-13 in solid amino-acids using the Cp-Mas technique, J. Magn. Reson. 54 (2) (1983) 226–235.
[13] N. Bloembergen, On the interaction of nuclear spins in a crystalline lattice, Physica 15 (3–4) (1949) 386–426.
[14] A. Abragam, The Principles of Nuclear Magnetism, first ed., Clarendon Press, Oxford, 1961.
[15] D. Suter, R.R. Ernst, Spin diffusion in resolved solid-state NMR-spectra, Phys. Rev. B 32 (9) (1985) 5608–5627.
[16] P.M. Henrichs, M. Linder, J.M. Hewitt, Dynamics of the C-13 spin-exchange process in solids—a theoretical and experimental-study, J. Chem. Phys. 85 (12) (1986) 7077–7086.
[17] B.H. Meier, Polarization transfer and spin diffusion in solid-state, Adv. Magn. Opt. Reson. 18 (1994) 1.
[18] N. Bloembergen, S. Shapiro, P.S. Pershan, J.O. Artman, Cross-relaxation in spin systems, Phys. Rev. 114 (2) (1959) 445–459.
[19] A. Kubo, C.A. McDowell, Spectral spin diffusion in polycrystalline solids under magic-angle spinning, J. Chem. Soc. Faraday Trans. I 84 (1988) 3713–3730.
[20] F. Castellani, B. van Rossum, A. Diehl, M. Schubert, K. Rehbein, H. Oschkinat, Structure of protein determined by solid-state magic-angle-spinning NMR spectroscopy, Nature 420 (2002) 98–102.
[21] A. Krushelnitsky, D. Reichert, Solid-state NMR and protein dynamics, Prog. Nucl. Magn. Reson. Spectrosc. 47 (1–2) (2005) 1–25.
[22] B. Reif, B.J. van Rossum, F. Castellani, K. Rehbein, A. Diehl, H. Oschkinat, Characterization of H-1–H-1 distances in a uniformly H-2,N-15-labeled SH3 domain by MAS solid-state NMR spectroscopy, J. Am. Chem. Soc. 125 (6) (2003) 1488–1489.
[23] B. Elena, L. Emsley, Powder crystallography by proton solid-state NMR spectroscopy, J. Am. Chem. Soc. 127 (25) (2005) 9140–9146.
[24] M. Juy, F. Penin, A. Favier, A. Galinier, R. Montserret, R. Haser, J. Deutscher, A. Böckmann, Dimerization of Crh by reversible 3D domain swapping induces structural adjustments to its monomeric homologue HPr, J. Mol. Biol. 332 (2003) 767–776.
[25] F. Castellani, B.J. van Rossum, A. Diehl, K. Rehbein, H. Oschkinat, Determination of solid-state NMR structures of proteins by means of three-dimensional N-15–C-13–C-13 dipolar correlation spectroscopy and chemical shift analysis, Biochemistry 42 (39) (2003) 11476–11483.
[26] A. Böckmann, A. Lange, A. Galinier, S. Luca, N. Giraud, M. Juy, H. Heise, R. Montserret, F. Penin, M. Baldus, Solid state NMR sequential resonance assignments and conformational analysis of the 2×104 kDa dimeric form of the *Bacillus subtilis* protein Crh, J. Biomol. NMR 27 (4) (2003) 323–339.
[27] S. Macura, R.R. Ernst, Elucidation of cross relaxation in liquids by two-dimensional NMR-spectroscopy, Mol. Phys. 41 (1) (1980) 95–117.
[28] A. Lange, K. Seidel, L. Verdier, S. Luca, M. Baldus, Analysis of proton–proton transfer dynamics in rotating solids and their use for 3D structure determination, J. Am. Chem. Soc. 125 (41) (2003) 12640–12648.
[29] Maplesoft Maple, 9.50, 2004.
[30] A. Lesage, A. Böckmann, Water–protein interactions in microcrystalline Crh measured by H-1–C-13 solid-state NMR spectroscopy, J. Am. Chem. Soc. 125 (44) (2003) 13336–13337.
[31] A. Böckmann, M. Juy, E. Bettler, L. Emsley, A. Galinier, F. Penin, A. Lesage, Water–protein hydrogen exchange in the micro-crystalline protein Crh as observed by solid state NMR spectroscopy, J. Biomol. NMR 32 (3) (2005) 195–207.
[32] A. Lesage, L. Emsley, F. Penin, A. Böckmann, Investigation of dipolar-mediated water–protein interactions in microcrystalline Crh by solid-state NMR spectroscopy, J. Am. Chem. Soc. 128 (25) (2006) 8246–8255.